CrossMark

ORIGINAL PAPER

Correlation between right ventricular T_1 mapping and right ventricular dysfunction in non-ischemic cardiomyopathy

Christine L. Jellis[1,2] · Teerapat Yingchoncharoen[1] · Neville Gai[3] · Kenya Kusunose[1] ·
Zoran B. Popović[1,2] · Scott Flamm[2] · Deborah Kwon[1,2]

Abstract Right ventricular (RV) fibrosis is increasingly recognized as the underlying pathological substrate in a variety of clinical conditions. We sought to employ cardiac magnetic resonance (CMR) techniques of strain imaging and longitudinal relaxation time (T_1) mapping to better examine the relationship between RV function and structure. Our aim was to initially evaluate the feasibility of these techniques to evaluate the right ventricle. We then sought to explore the relationship between RV function and underlying fibrosis, along with examining the evolution of RV remodeling according to the amount of baseline fibrosis. Echocardiography was performed in 102 subjects with non-ischemic cardiomyopathy. Right ventricular parameters were assessed including: fractional area change (FAC) and longitudinal strain. The same cohort underwent CMR. Post-contrast T_1 mapping was performed as a marker of fibrosis with a Look-Locker technique using inversion recovery imaging. Mid-ventricular post-contrast T_1 values of the RV free wall, RV septum and lateral LV were calculated using prototype analysis software. Biventricular volumetric data including ejection fraction was measured by CMR using a cine short axis stack. CMR strain analysis was also performed to assess 2D RV longitudinal and radial strain. Simultaneous biochemical and anthropometric data were recorded. Subjects were followed over a median time of 29 months (IQR 20–37 months) with echocardiography

to evaluate temporal change in RV FAC according to baseline post-contrast T_1 values. Longitudinal data analysis was performed to adjust for patient loss during follow-up. Subjects (62% men, 51 ± 15 years) had mild to moderately impaired global RV systolic function (RVEF = $39 \pm 15\%$; RVEDV = 187 ± 69 ml; RVESV = 119 ± 68 ml) and moderate left ventricular dysfunction at baseline (LVEF $30 \pm 17\%$). Good correlation was observed between mean LV and RV post-contrast T_1 values (r = 0.652, p < 0.001), with similar post-contrast T_1 values maintained in both the RV free wall and septum (r = 0.761, p < 0.001). CMR RVEF demonstrated a proportional correlation with echocardiographic measures of RV longitudinal function and CMR RV strain (longitudinal r = −0.449, p = 0.001; radial r = −0.549, p < 0.001). RVEF was related to RV post-contrast T_1 values, particularly in those with RV dysfunction (free wall T_1 r = 0.259 p = 0.027; septal T_1 r = 0.421 p < 0.001). RV strain was also related to RV post-contrast T_1 values (r = −0.417, p = 0.002). Linear regression analysis demonstrated strain and post-contrast T1 values to be independently associated with RVEF. Subjects with severe RV dysfunction (CMR RVEF <25%) demonstrated lower RV CMR strain (longitudinal p = 0.018; radial p < 0.001), RV T_1 values (free wall p = 0.013; septum <0.001) and RV longitudinal echocardiography parameters despite no difference in afterload. During follow-up, those with RV free wall post-contrast T_1 values ≥ 350 ms demonstrated ongoing improvement in FAC ($\Delta 6\%$), whilst values <350 ms were associated with deterioration in RV function ($\Delta FAC = −5\%$) (p = 0.026). CMR provides a comprehensive method by which to evaluate right ventricular function. Post-contrast T_1 mapping and CMR strain imaging are technically feasible and provide incremental information regarding global RV function and structure. The proportional relationship between RV function and post-contrast T_1 values supports that myocardial

✉ Christine L. Jellis
jellisc@ccf.org

1 Department of Cardiovascular Medicine, Desk J1-5, Heart and Vascular Institute, Cleveland Clinic, 9500 Euclid Avenue, Cleveland, OH 44195, USA

2 Imaging Institute Cleveland Clinic, Cleveland, OH, USA

3 National Institutes of Health, Bethesda, MD, USA

🙲 Springer

fibrosis is a causative factor of RV dysfunction in NICM, irrespective of RV afterload. This same structural milieu also appears integral to the propensity for both positive and negative RV remodeling long-term, suggestive that this is also determined by the degree of underlying RV fibrosis.

Introduction

Left ventricular (LV) longitudinal relaxation time (T_1) mapping is increasingly employed for assessment of diffuse myocardial fibrosis in a variety of non-ischemic cardiomyopathies including: hypertensive heart disease, hypertrophic cardiomyopathy (HCM), idiopathic dilated cardiomyopathy (DCM), infiltrative cardiomyopathy and metabolic processes such as diabetes [1–3]. Post-contrast T_1 values have been previously validated against endomyocardial biopsy, therefore enabling non-invasive quantification of diffuse myocardial fibrosis, without the inherent limitations of delayed enhancement imaging, where normal myocardium is required for contrasting signal intensity [4]. Post-contrast T_1 values have also been inversely correlated with both LV systolic and diastolic function, with additional LV clinical applications further rapidly expanding for this useful technique [3, 5].

In contrast, there is limited corresponding knowledge regarding the relationship between right ventricular (RV) structure, fibrosis and systolic function, despite RV fibrosis increasingly being recognized as an underlying pathological substrate in a variety of clinical conditions including: arrhythmogenic right ventricular cardiomyopathy, pulmonary hypertension and ultra-endurance athlete's heart [6–8]. This underlying fibrosis is thought to predispose to clinical sequelae including: arrhythmias, heart failure and impaired functional capacity. RV function is also challenging to quantitate as the asymmetrical RV shape precludes many of the echocardiographic geometrical assumptions made for evaluation of the left ventricle. This is reflected by the multiple RV echocardiography parameters required in combination for assessment, with resultant determinants of global RV function made using limited parameters such as fractional area change (FAC) and markers of RV free wall longitudinal motion.

Cardiac magnetic resonance imaging (CMR) has enables more accurate quantification of RV volumes and global function than echocardiography. It is now the gold standard for calculation of these RV parameters [9]. In addition to the calculation of ejection fraction, the improved ability to reconstruct the RV in three dimensions should also lend itself to better assessment of RV free wall function in multiple tissue planes. In theory this should now enable calculation of global and regional RV strain in both longitudinal and radial planes to allow for more comprehensive evaluation of overall RV function. As yet, CMR T_1 mapping has had limited adoption for assessment of RV structure and underlying fibrosis, although preliminary small number data appears promising [10]. Endomyocardial biopsy of the RV is commonly performed; however tissue is typically taken from the RV aspect of the interventricular septum, rather than the RV free wall to reduce the risk for perforation and cardiac tamponade [11]. Hence, evaluation and quantification of fibrosis within the RV free wall remains limited.

We sought to incorporate the CMR techniques of post-contrast T_1 mapping (as a marker of fibrosis) and strain imaging to better evaluate RV structure and function respectively. Our aim was to initially evaluate the feasibility of performance of these techniques on the right ventricle. We then sought to explore the relationship between RV function, remodeling and fibrosis according to these CMR variables and other standard echocardiographic measures. Lastly, we aimed to explore the evolution of RV function using these same parameters. Our hypotheses were that RV post-contrast T_1 mapping and strain techniques would be technically feasible and that there would be correlation between non-invasive quantitative physiological markers of RV function and structure.

Methods

We retrospectively reviewed 102 consecutive subjects with non-ischemic cardiomyopathy (NICM), who were referred for and successfully completed both CMR and transthoracic echocardiography. Subjects with NICM were selected to provide a wide range of biventricular function for analysis. Subjects were excluded if image quality using either modality was suboptimal for image analysis, including adequate frame rate and tissue tracking for echocardiography deformation imaging. NICM was defined as a history of impaired left ventricular systolic dysfunction with LVEF <50% and no other causes of cardiomyopathy including: ischemic, valvular, hypertensive or congenital heart disease. Approval for this study was granted by the Institutional Review Board of the Cleveland Clinic Foundation, Main Campus, Cleveland, Ohio.

Demographic, anthropometric, and metabolic data

Clinical data were collected regarding subject age, gender, anthropometry, biochemistry (including creatinine) and hematocrit (Table 1).

Table 1 Subject characteristics at baseline

Subject characteristics at baseline	Mean value (±SD), percentage (%) or median (IQR)
Age (years)	51 ± 15
Gender (male)	62%
Weight (kg)	87 ± 20
Height (m)	174 ± 11
BSA (m^2)	3.0 ± 0.4
BMI (kg/m^2)	29 ± 6
Heart rate (bpm)	80 ± 21
Systolic blood pressure (mmHg)	108 ± 20
Glomerular filtration rate (ml/min)	87 (72–117)
Hematocrit (%)	39.6 ± 5.5
Angiotensin converting enzyme inhibitor use	63%
Angiotensin 2 receptor blocker use	16%
Beta-blocker use	84%
Aldosterone antagonist use	31%
Loop diuretic use	49%
Statin use	33%

Echocardiography

A commercially available cardiac ultrasound machine (Vivid 7/e9; General Electric Medical Systems, Milwaukee, WI) was used to perform a comprehensive resting echocardiogram. Left ventricular systolic function was assessed using the modified Simpson biplane method for volumetric analysis and subsequent calculation of LVEF. Color and spectral Doppler imaging was performed to assess valvular morphology and exclude significant underlying valvular disease. Additionally, subjects underwent dedicated echocardiographic assessment of the RV including: RV optimized 2D imaging, measurement of RV FAC, M-mode imaging to determine RV free wall tricuspid annular plane of systolic excursion (TAPSE), spectral Doppler imaging to estimate RV systolic pressure (RVSP) from the peak tricuspid regurgitant velocity and RV free wall longitudinal systolic tissue velocity (RV s') via color tissue Doppler imaging. Apical long-axis images were captured with suitable frame rates (50–75/s) for performance of offline 2D strain imaging. Strain analysis was performed with commercially available software (EchoPac; GE Vingmed, Horten, Norway). Semi-automated 2D longitudinal deformation imaging was performed by tracing the RV myocardium on an RV optimized apical 4 chamber view. Global mean peak RV strain was determined, which included both the RV free wall and interventricular septum. Peak RV free wall strain was also calculated by averaging the peak strain values from the three free wall segments. Subjects were then followed with serial echocardiograms to evaluate temporal change in RV FAC.

CMR imaging

All subjects underwent CMR imaging on a 1.5 T Achieva scanner (Philips Healthcare, Cleveland, OH) with vectorcardiogram (VCG) gating, a dedicated 8-channel cardiac surface coil, and inspiratory breath holds. Turbo spin echocardiography and gradient echocardiography imaging for anatomic definition were performed. After the cardiac axes were determined with localizers, vertical (VLA) and horizontal long-axis (HLA) and short-axis cine MRI was performed with a balanced steady-state free-procession sequence for cardiac chamber quantification, wall motion assessment and valvular analysis. Short-axis slice thickness was 8 mm. Biventricular CMR volumetric data was measured off-line (CVI^{42}, Circle Cardiovascular Imaging Inc., Calgary, Canada) using the cine short axis stack to establish LV and RV end-diastolic volumes (EDV), end-systolic volumes (ESV) and biventricular ejection fractions (EF). Normal RV ejection fraction by CMR was defined as $\geq 50\%$ [12, 13].

Gadolinium based contrast (Magnevist, Bayer, HealthCare, Whippany, USA) was administered, and 15 min later, post-contrast imaging was performed with an inversion recovery Look-Locker technique in a standard short-axis slice at the mid-ventricular cavity level. Slice thickness was maintained at 10 mm. Imaging parameters were: repetition time (TR)/echo time(TE): 4.0/1.8 ms, flip angle (FA): 45°, acquisition matrix (Acq matrix): 256×160 pixels, and field of view (FOV): 38 cm. Subsequently, standard late gadolinium enhancement (LGE) imaging was then performed in the LV short axis and long axis planes with

an inversion-recovery sequence with the inversion time set to null normal myocardium [slice thickness: 8 mm, Acq matrix 256×160 pixels, FOV: 40 m, number of excitations (NEX): 2]. Evaluation for focal LGE was performed, to assess for underlying scar in either ventricle.

The Look-Locker technique involved VCG gating and a single breath hold technique. Approximately 20 images, each with a consecutively longer inversion time, were acquired at the mid-ventricular level. Offline, regions of interest (ROI) were manually traced on each short axis image. These ROI were specifically placed within the mid RV free wall (orange), RV blood pool (aqua), mid RV septum (yellow) and mid LV lateral wall (blue) using proto-type CVI42 software. When tracing the myocardial ROI, care was taken to avoid regions of LGE, non-myocardial structures, trabeculations and adjacent blood pool (Fig. 1).

Signal intensities were then measured within each of the 4 ROI at the incrementally longer inversion times.

Exponential recovery curves of these values were then generated on a pixel-by-pixel basis for each designated ROI from which the regional myocardial post-contrast T_1 times could be extrapolated as a marker of myocardial fibrosis (Fig. 2). The T_1 constant that is obtained directly from the fit is referred to as T_1^*. A three parameter model $[A - B.\exp(-TI/T_1^*)]$ was used for curve fitting and T_1 was determined using $T_1 = (B/A - 1).T_1^*$. An automated
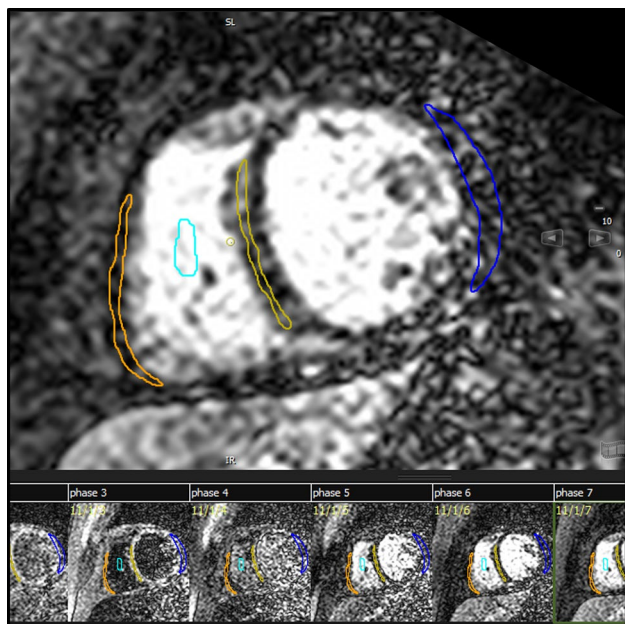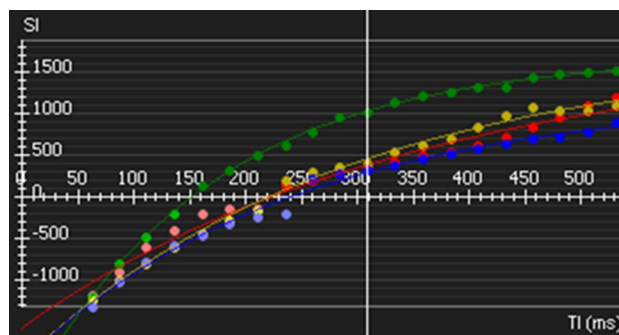
Fig. 2 Signal intensity time curves were extrapolated for each of the 4 regions of interest at incrementally longer inversion times. These exponential recovery curves were employed to determine regional myocardial post-contrast T_1 times [mid RV free wall (*red*), RV blood pool (*green*), mid RV septum (*yellow*) and mid LV lateral wall (*blue*)]

curve-fitting technique was also used to generate a post-contrast T_1 map based upon the premise that a shorter post-contrast T_1 time corresponds to increased gadolinium retention and greater extra-cellular volume such as fibrosis. Several physiological confounders can impact upon post-contrast T_1 values. As such, raw post-contrast T_1 values were adjusted for estimated glomerular filtration rate (eGFR), body size, gadolinium dose and post-contrast delay time based on an analytical solution to a kinetic model [14]. Regional post-contrast T1 relaxation times for the RV and LV were then compared between subjects.

CMR strain analysis was performed to measure global 2D biventricular longitudinal (GLS) and RV radial strain (GRS) using commercially available software (TomTec Imaging Systems Corp, Munich, Germany). This involved employing a semi-automated tissue tracking algorithm to track myocardial deformation throughout the cardiac cycle on standard cine SSFP images. Manual adjustments were made to ensure optimal and appropriate myocardial tracking as required. Peak 2D longitudinal strain was measured from the three standard apical long axis planes and averaged to determine LV GLS. RV peak strain was determined from a horizontal long-axis cine image. Peak RV GLS strain was calculated as the mean peak strain including all segments of the RV free wall and inter-ventricular septum (Fig. 3). Mean peak RV longitudinal free wall strain was defined as the mean peak strain of the three RV free wall segments. RV radial strain was measured in a similar fashion in 6 short axis segments from a mid-ventricular level cine short axis image. The mean peak value for each of the six segments was determined and averaged to calculate RV GRS (Fig. 4).
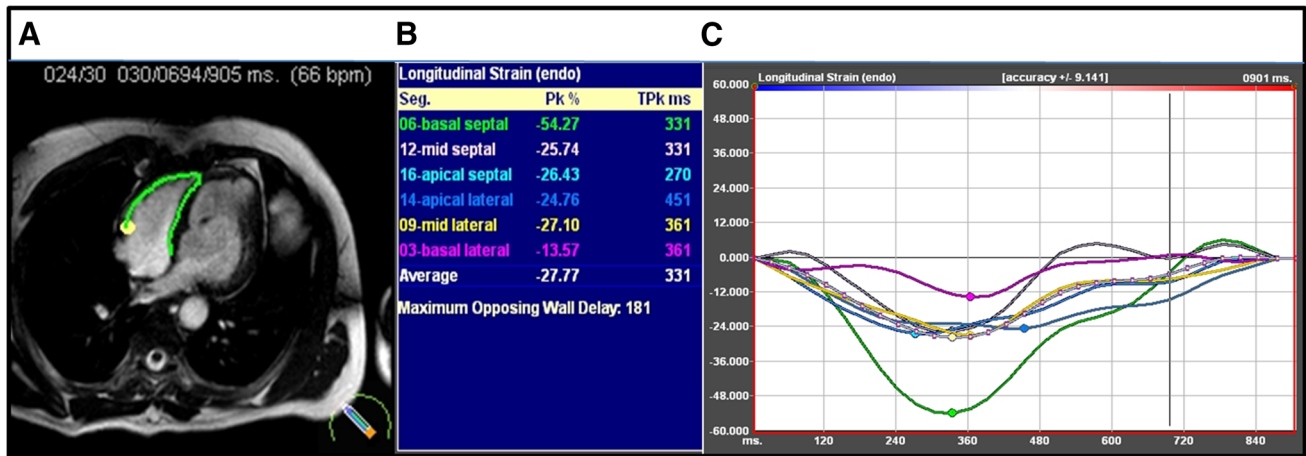

Fig. 1 Regional post-contrast T_1 values were determined offline by manually tracing regions of interest (ROI) on the short axis cardiac magnetic resonance images at the mid ventricular level. These ROIs were specifically placed within the mid RV free wall (*orange*), RV blood pool (*aqua*), mid RV septum (*yellow*) and mid LV lateral wall (*blue*) using prototype analysis software

Fig. 3 Right ventricular longitudinal strain cardiac magnetic resonance strain analysis was performed offline using a semi-automated tissue tracking algorithm to track myocardial deformation throughout the cardiac cycle on a horizontal long axis cine image (**a**) and determine regional and global peak right ventricular 2D longitudinal strain (**b, c**). From this, mean peak RV free wall was defined as the mean peak longitudinal strain of the three right ventricular free wall segments
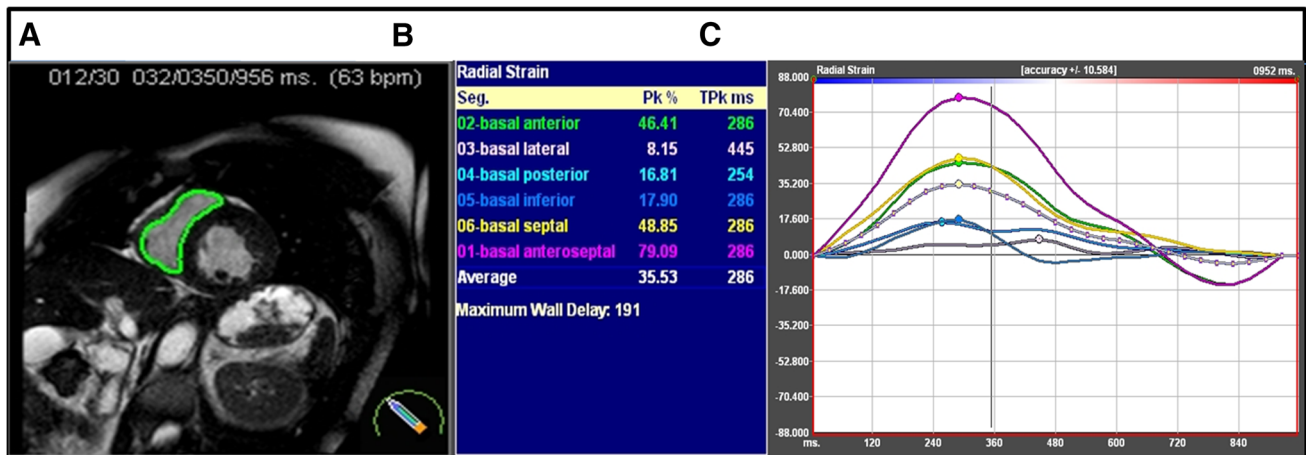
Fig. 4 Right ventricular radial strain cardiac magnetic resonance strain analysis was performed offline using a semi-automated tissue tracking algorithm to track myocardial deformation throughout the cardiac cycle on a mid-ventricular level cine short axis image (**a**). The mean peak value for each of the six segments was determined (**b, c**) and averaged to calculate right ventricular global radial strain

Statistical analysis

Results are expressed as mean and standard deviation (SD), median and interquartile range (IQR) or subject number and percentage. The normality of continuous data was verified with a Kolmogorov–Smirnov test. Analysis of normally distributed variables was performed with Pearson bivariate correlations, whilst nonparametric variables were analyzed using Spearman correlations. Comparison of groups was performed using independent T-tests. Independent associations were sought with linear and logistic regression models of independent variables. Candidate variables for the models were selected on clinical grounds, guided by univariable correlation with p value <0.10 and

the absence of colinearity. Longitudinal data analysis was performed to adjust for patient loss during follow-up. Statistical analysis was performed with standard statistical computer software (SPSS 17; SPSS Inc, Chicago, Illinois). $p < 0.05$ was deemed to be statistically significant.

Results

Subjects (51 ± 15 years, 62% male) were overweight (BMI 29 ± 6 kg/m^2), but had normal renal function (median eGFR 87 ml/min, IQR 72–117) and hematocrit ($39.6 \pm 5.5\%$). The proportion of subjects on recommended heart failure therapy was high, with 79% of subjects on an angiotensin

converting enzyme inhibitor or angiotensin 2 receptor blocker and 84% on beta-blockers at baseline (Table 1). Baseline echocardiography and CMR were performed 6 ± 139 days apart on average.

CMR—volumetric data

Volumetric analysis by CMR demonstrated that left ventricular function was moderately reduced overall (LVEF $30 \pm 17\%$), with increased LV volumes (EDV 276 ± 102 ml; ESV 201 ± 102 ml) but normal LV mass (145 ± 48 g). These results were consistent with the pre-specified inclusion criteria of non-ischemic cardiomyopathy. Right ventricular systolic function was concurrently noted to be mild to moderately impaired (mean RVEF = $39 \pm 15\%$), with associated right ventricular enlargement (RVEDV = 187 ± 69 ml; RVESV = 119 ± 68 ml). RVEF modestly correlated with LVEF. There were 74 (73%) study subjects with RV dysfunction (Table 2).

CMR—strain data

CMR GLS for the LV was moderately reduced globally, without significant regional variation. This was also consistent with NICM and the documented moderately reduced LVEF. LV 2D GLS strain was $-10.9 \pm 5.0\%$ and remained similar when analyzed regionally (HLA [4 chamber] view $-10.9 \pm 5.2\%$, VLA [2 chamber] view $-10.8 \pm 5.8\%$ and long-axis [3 chamber] $-11.1 \pm 5.9\%$). RV free wall longitudinal strain was at least mildly reduced globally ($-20.0 \pm 6.9\%$), with an expected progressive reduction regionally moving from base to apex, likely related to greater apical tethering (basal segment $-23.2 \pm 12.0\%$, mid segment $-20.0 \pm 9.1\%$, apical segment $-16.9 \pm 9.3\%$).

RV GLS incorporated mean strain from the RV free wall and interventricular septum and was moderately reduced ($-12.5 \pm 5.9\%$) in comparison to free wall strain. However, this disparity likely reflects the predominant contribution of LV function to deformation of the interventricular septum. RV GRS was reduced at $-7.4 \pm 3.6\%$. Although, normal values for this parameter are not yet defined.

CMR—post-contrast T$_1$ mapping

Focal LGE within the left ventricle was identified in 45 patients (44%), however no subjects had focal enhancement of the RV free wall. Mean RV free-wall and septal post-contrast T$_1$ values were similar to LV values overall, with good correlation demonstrated between RV free wall post-contrast T1 values and those measured in the RV septum and LV lateral wall, consistent with an underlying global process (Fig. 5a, b). Bland Altman analysis examining the difference between post-contrast T1 values in the RV free wall compared with the septum and LV lateral wall demonstrated a relatively even spread of data around the mean for both comparisons (Fig. 5c, d). Post-contrast (raw, uncorrected) T$_1$ results were 350 ± 66 ms for the RV free wall, 359 ± 74 ms for the RV septum and 384 ± 78 ms for the LV lateral wall. Corrected post-contrast T$_1$ values were still relatively similar at 377 ± 73 ms for the RV free wall, 390 ± 74 ms for the RV septum and 414 ± 87 ms for the LV lateral wall. These results compare to a previously published post-contrast T$_1$ value for the left ventricle in NICM of 439 ms (397–483 ms) [15]. However, inter-study comparison of post-contrast T$_1$ values can be influenced by scanner, mapping technique and type and dose of contrast media even despite our intra-study corrections of raw data for individual patient confounding factors. Normal values

Table 2 Bivariate correlations between CMR right ventricular ejection fraction and other parameters of right ventricular structure and biventricular function for the whole study population and for those with right ventricular dysfunction (RVEF <50%)

	Whole study population (n = 102)			Subjects with RV dysfunction (n = 74)		
	Mean ± SD	r	p	Mean ± SD	r	p
Left ventricular CMR ejection fraction (%)	30 ± 17	0.353	<0.001	29 ± 18	0.392	0.001
Right ventricular free wall post-contrast T$_1$ (ms)	378 ± 73	0.018	0.859	384 ± 79	0.259	0.027
Right ventricular septal post-contrast T$_1$ (ms)	359 ± 74	0.199	0.045	392 ± 75	0.421	<0.001
Left ventricular lateral wall post-contrast T$_1$ (ms)	414 ± 87	0.265	0.007	409 ± 94	0.344	0.003
Right ventricular systolic pressure (mmHg)	37 ± 14	−0.245	0.040	41 ± 16	−0.573	0.066
Tricuspid annular plane of systolic excursion [TAPSE] (cm)	2.0 ± 0.7	0.358	0.001	1.9 ± 0.6	0.490	<0.001
Right ventricular systolic tissue velocity [s'] (cm/s)	10.9 ± 3.4	0.412	0.001	10.3 ± 3.2	0.230	0.134
Right ventricular CMR global longitudinal strain (%)	−12.5 ± 5.9	−0.449	0.001	−11.8 ± 5.3	−0.517	0.001
Right ventricular CMR free wall longitudinal strain (%)	−20.0 ± 6.9	−0.402	0.003	−18.9 ± 6.1	−0.286	0.077
Right ventricular CMR global radial strain (%)	−7.4 ± 3.6	−0.549	<0.001	−6.8 ± 3.6	−0.563	<0.001
Left ventricular CMR global longitudinal strain (%)	−10.9 ± 5.0	−0.492	<0.001	−10.4 ± 4.9	−0.600	<0.001
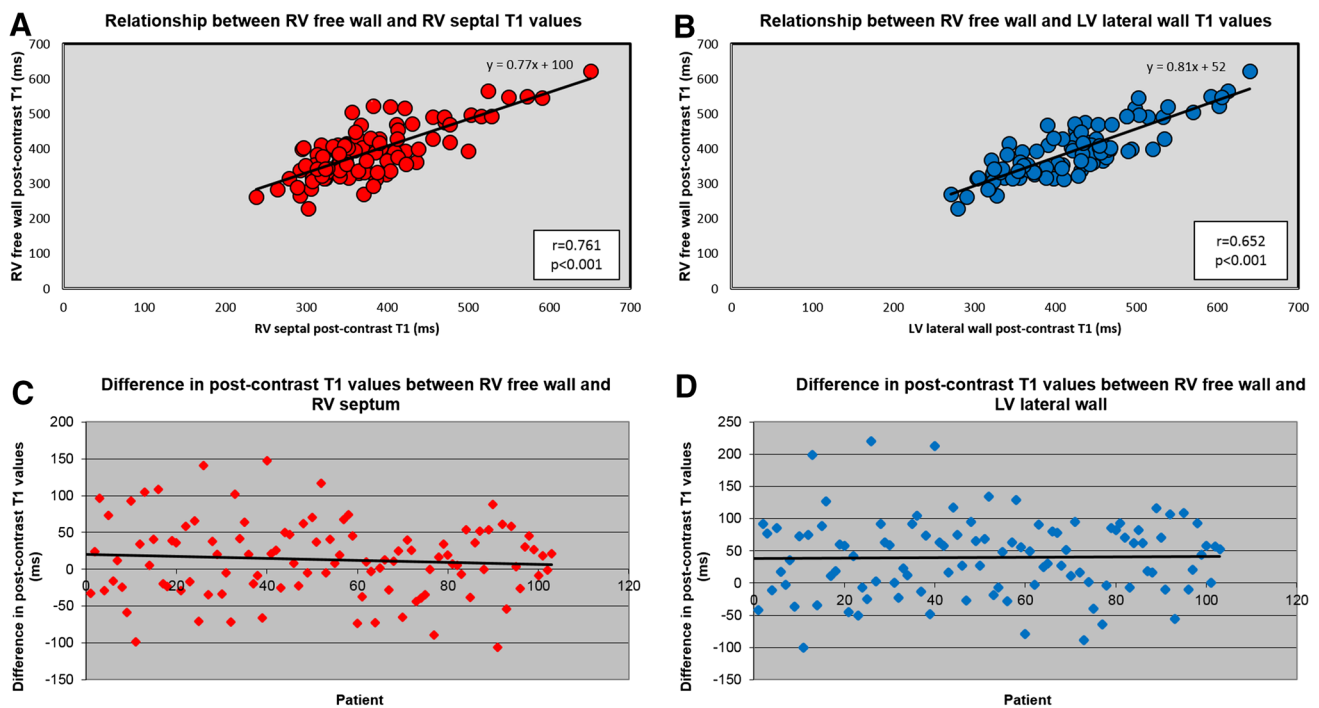
Fig. 5 Comparison of right ventricular (RV) free wall post-contrast T_1 values with RV free wall and left ventricular (LV) lateral wall post-contrast T_1 values: **a** correlation between mean RV free-wall and RV septal post-contrast T_1 values, **b** correlation between mean RV free-wall and LV lateral wall post-contrast T_1 values, **c** Bland Altman analysis comparing the difference between RV free-wall and RV septal post-contrast T_1 values, **d** Bland Altman analysis comparing the difference between RV free-wall and LV lateral wall post-contrast T_1 values

for right ventricular post-contrast T_1 values have not been defined, but are presumably similar to LV values in a normal heart.

Echocardiography—RV parameters

RV FAC by echocardiography demonstrated normal mean RV function when averaged for the whole study population, with a mean FAC of $42 \pm 9\%$ (normal >35%) [16]. Other echocardiographic parameters of RV function were also preserved, although predominantly reflect basal free wall longitudinal function. These include RV s' (10.9 ± 3.4 cm/s) and TAPSE (2.0 ± 0.7 cm). Overall, right heart pressures were not significantly elevated when estimated by echocardiography, as reflected by a peak tricuspid regurgitant velocity of 2.5 ± 0.5 m/s and corresponding RVSP of 37 mmHg. 2D longitudinal strain imaging by echocardiography reflected similar RV strain findings to the CMR results, despite different analysis software. Free wall RV longitudinal strain was $-18.9 \pm 6.8\%$, with the same gradient noted between basal and apical segments (basal segment $-20.9 \pm 7.7\%$, mid segment $-20.0 \pm 7.5\%$, apical segment $-15.8 \pm 8.8\%$).

Correlation between CMR and echocardiography

There was no difference in LVEF when measured by echocardiography compared with CMR (32 ± 11 vs. $30 \pm 17\%$, $p = 0.2$), although as expected CMR volumes were proportionally increased (CMR LVEDV 277 ± 103 ml, LVESV 202 ± 103 ml; Echocardiography LVEDV 181 ± 78 ml, LVESV 124 ± 71 ml). LV 2D GLS results were also similar by echocardiography (-8.5 ± 2.8), compared with CMR (-10.1 ± 4.1) and correlated well ($r = 0.795$, $p < 0.001$). Likewise, echocardiography and CMR strain demonstrated moderate concordance for RV strain (free wall strain -18.9 ± 6.8 vs. $-20.0 \pm 6.9\%$, $r = -0.42$, $p = 0.074$). RVEF by CMR demonstrated a proportional correlation with echocardiography measures of RV longitudinal function, including TAPSE and RV s'. When selected for abnormal RVEF, those with RV dysfunction had predictably lower TAPSE and RV s' values, along with a higher RVSP (Table 2). RV strain by both CMR and echocardiography demonstrated an inverse relationship with RVEF. Specifically, a lower RVEF was associated with smaller (less negative) strain values, especially amongst those with abnormal RV function (Table 2).

Relationship between RV function and structure

RVEF was proportionally related to multiple markers of RV function and also to myocardial structure as represented by RV post-contrast T_1 values (Table 2). On multivariate linear regression analysis of these significant univariate correlates within the whole study population, RV CMR GLS (ß=−0.674, p=0.018) and RV septal post-contrast T_1 values (ß=0.482, p=0.070) were most independently associated with RVEF. When analysis was limited to subjects with RV dysfunction, an even stronger relationship between RVEF and both post-contrast T1 values and other parameters of RV dysfunction was noted. Multivariate linear regression analysis of univariate correlates within this sub-population also demonstrated RVEF to be independently associated with RV free wall post-contrast T_1 (ß=0.447, p=0.040) and RV CMR GLS (ß=−0.559, p=0.030). Thereby supportive that myocardial fibrosis plays a causative role in the RV dysfunction manifested in NICM.

When subjects were further stratified according to severity of RV dysfunction, subjects with severe RV dysfunction (CMR RVEF <25%) demonstrated lower strain, post-contrast T_1 values and TAPSE despite no difference in afterload (as measured by RVSP) (Table 3). Although RVSP did not correlate with post-contrast T_1 values, there was a relationship noted between RVSP and RV free wall strain (r=−0.363, p=0.041). RV free wall strain was also related to RV free wall post-contrast T_1 values (r=−0.417, p=0.002), further supportive of the link between RV function and structure.

Lastly, subjects were dichotomized based upon RV free wall post-contrast T_1 values of above or below 350 ms as this approximated the median RV free wall post-contrast T_1 value for the population (363 ms) and this cut-point was felt to be a good identifier of those with clearly abnormal post-contrast T_1 values (based upon previously defined normal post-contrast T_1 values for the LV) [17]. Those with lower

baseline post-contrast T_1 values (<350 ms) had reduced RV free wall CMR strain (−18±6 vs. −23±7%; p=0.007), but otherwise similar baseline parameters including: age, renal function, weight, RVEF, LVEF and echocardiography parameters (FAC, RVSP and TAPSE). When subjects were followed over a median time of 29 months (IQR 20–37) with echocardiography, those with RV free wall post-contrast T_1 time ≥350 ms demonstrated a significant ΔFAC of 6% compared to those with post-contrast T_1 values <350 ms who demonstrated a progressive deterioration in RV function over time (ΔFAC=−5%) (p=0.026) (Fig. 6).

Discussion

The asymmetrical geometry of the right ventricle has made it traditionally difficult to quantitate using 2D echocardiography and standard acoustic windows. As such, in most clinical imaging laboratories, assessment of RV function
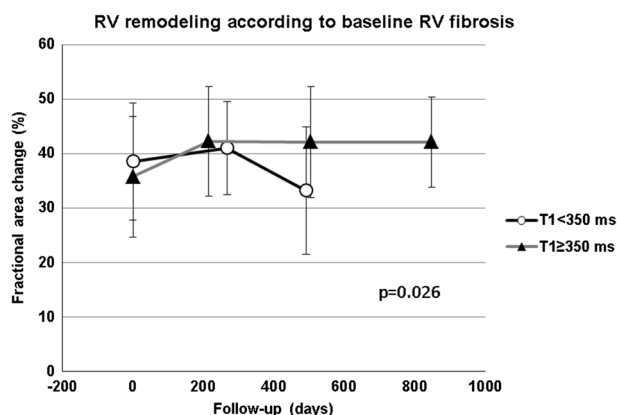
Fig. 6 Right ventricular remodeling [measured by fractional area change (FAC)] according to the degree of baseline right ventricular fibrosis (post-contrast T_1 </≥ 350 ms)

Table 3 T-test comparing parameters of right ventricular function and structure, in study subjects stratified according to severe or non-severe baseline right ventricular impairment

	RVEF < 25% (n = 19; 16 ± 6%) Mean ± SD	RVEF ≥ 25% (n = 83; 45 ± 11%) Mean ± SD	p
Right ventricular free wall post-contrast T_1 (ms)	339 ± 52	385 ± 75	0.013
Right ventricular septal post-contrast T_1 (ms)	336 ± 50	403 ± 74	<0.001
Left ventricular lateral post-contrast T_1 (ms)	349 ± 46	428 ± 87	<0.001
Right ventricular global longitudinal strain (%)	−8.9 ± 4.4	−13.5 ± 5.9	0.018
Right ventricular global radial strain (%)	−3.9 ± 1.9	−8.3 ± 3.3	<0.001
Left ventricular global longitudinal strain (%)	−6.4 ± 4.0	−12.1 ± 4.6	<0.001
Left ventricular ejection fraction (%)	17 ± 7	33 ± 17	<0.001
Tricuspid annular plane of systolic excursion [TAPSE] (cm)	1.5 ± 0.4	2.1 ± 0.7	0.004
Right ventricular systolic tissue velocity [s'] (cm/s)	10 ± 3	11 ± 3	0.298
Right ventricular systolic pressure (mmHg)	39 ± 12	36 ± 14	0.440

has remained largely qualitative and in many cases there is rudimentary or minimal evaluation at all. CMR heralds a new era of 3D/4D cardiac imaging, which is not limited by tissue planes and hence is ideally placed to revolutionize the way in which we visualize and evaluate the right ventricle. It has the potential to provide incremental quantitative data about RV function and structure, thereby reinventing our understanding of this critical structure. The clinical impact of this better understanding of the RV could be profound and has the potential to directly influence patient care via more accurate diagnosis, thereby facilitating institution of targeted appropriate therapy and potentially improved patient outcomes.

However, like every new application, RV CMR imaging must prove its technical feasibility to provide meaningful clinical data. This is particularly important for the RV, as not all LV validated measures can be automatically and appropriately extrapolated and applied to the RV. This relates predominantly to the inherent differences in structure between the RV and LV. In particular, the asymmetrical RV shape, its relatively thin free wall and the prominence of RV myocardial trabeculation can all result in technical limitations. Reassuringly, the performance of RV CMR parameters within this study all proved technically feasible. All patients had suitable image quality for data analysis and provided that ROI contours were drawn appropriately within the relatively thin RV free wall, meaningful post-contrast T_1 mapping offline analysis was able to be performed in all subjects. Specifically, particular care was taken to avoid contaminating the myocardial segmentations with blood pool, thereby resulting in a partial volume effect which would have artificially reduced post-contrast T_1 values. Care was also taken to place the septal ROI within the RV aspect of the interventricular septum, to try to maximize the likelihood that obtained post-contrast T_1 values reflected RV myocardial signal intensity, rather than simply that of the LV.

The inherent caution required to ensure that each ROI was appropriately placed overlying RV myocardium (and not blood pool or LV septum) on each image frame did require manual optimization in many patients. This detracted from the automaticity of the offline analysis technique and increased study processing time, although likely ensured better accuracy of results. Ideally as automated tissue tracking computer algorithms continue to improve, this will be less of an issue and this type of labor intensive manual processing will be reduced. Good agreement between regional RV and LV post-contrast T_1 values supports the consistency and internal validity of the biventricular post-contrast T_1 mapping technique in subjects with a global process such as NICM. Although high subject numbers are not necessarily required for a feasibility study, our inclusion of >100 subjects is substantially more than the previously published small study manuscript and abstracts in this area, which have each been limited to ≤24 participants [10, 18, 19]. We feel that our larger study numbers are important to provide a broad enough study population in which to test a potentially challenging technique such as RV post-contrast T1 mapping.

Within our cohort of subjects, there was good correlation demonstrated between CMR and echocardiographic quantitative markers of RV function and structure. Although not the focus of the study, LV evaluation was also reassuringly similar between modalities, further validating the usefulness of this multi-modality approach. Increased LV volumes were noted on CMR compared with echocardiography, in line with previous observations [20]. However, as this, proportionally occurred for both LVEDV and LVESV, it did not impact upon overall LVEF, which were similar between modalities. RV functional data demonstrated a proportional relationship between impaired RVEF and reductions in other parameters of RV longitudinal function including RV s' and TAPSE. Our data also demonstrated that CMR strain analysis provides complementary RV functional assessment to RVEF and echocardiography derived measures of RV performance. RV strain by echocardiography and CMR were similar for GLS, with incremental functional information facilitated by CMR using GRS. When stratified by degree of RV impairment according to RVEF, there was a consistent relationship between RVEF and all different types of strain. Specifically, those with reduced RVEF also had consistently reduced (less negative) longitudinal and radial strain. Hence, multiplanar strain via CMR provides incremental information over and above echocardiographic functional measures, which primarily are limited to assessment of free wall longitudinal function. These parameters include: echocardiography derived 2D strain, TAPSE and RV s'. Often these measures of longitudinal function can remain preserved, despite reduced radial contractility, thereby masking the true degree of RV dysfunction. This is illustrated in Table 2, where those with RV dysfunction (n=74, RVEF <50%) have low-normal TAPSE and s' results, which are only slightly worse than the whole study population. In contrast, a larger reduction in RV GRS within this sub-population is noted. This regional disparity is particularly important to recognize as it is the radial motion of the RV free wall, which is the main determinant of RV output. A small reduction in RV radial function can therefore have a significant impact on RV function and cardiac output, in the same way that a fireplace bellows exploits a small amount of radial movement to achieve a large amount of air movement through the device.

There has been a recent concerted effort to standardize left ventricular strain values between vendors so that consistent normal values can be published and accepted

within both research studies and clinical applications [21]. Whilst, this technique standardization should also impact upon the reproducibility of RV strain between vendors, this is yet to be formally validated and a consensus for multi-vendor normal values for RV strain remains unpublished. Similarly, it is likely that there is some disparity between MRI strain between different vendors and software analysis packages. Normal values for MRI biventricular strain also remain undefined. Although the good correlation between echocardiography and MRI strain in this paper is reassuring, MRI normal strain results must formally be established and then their relationship with echocardiography strain determined, before multimodality strain can be extrapolated into clinical use and direct comparison between both techniques can be instituted with confidence. There are also two methods by which RV longitudinal strain can be measured. This involves either RV free wall strain (3 free wall segments) or global strain (3 free wall and 3 septal segments). Typically RV free wall strain results are higher than global strain results, due to the piston-like action of the unrestricted RV free wall. In contrast, global RV strain measures can be impacted by tethering of the RV to the LV and underlying LV dysfunction, which may result in comparatively lower strain results. This obviously impacts upon the resultant strain and was why we chose to report both free wall and global RV strain values in this paper. A consensus regarding the most appropriate convention is still to be determined. Most echocardiography and CMR strain analysis software packages also do not have dedicated measurement tools for evaluation of RV strain. Hence, most RV strain is actually measured using repurposed LV strain analysis tools and 'tricking' the software into tracking the RV instead of the LV. Dedicated RV analysis software is in evolution and will hopefully ameliorate this situation and provide more dedicated and consistent evaluation of RV function.

Limitations

Although the apparent deterioration of RV function with time (as measured by FAC) in subjects with post-contrast T_1 values <350 ms is suggestive of baseline fibrosis playing a progressively detrimental role in RV mechanics, cause cannot be attributed based upon these non-invasive findings especially in a population with relatively preserved FAC results at baseline. However, similar findings within this same cohort linking baseline LV post-contrast T_1 values to adverse remodeling of the LV over time is reassuring [22]. Although FAC is currently recommended as a method of choice for evaluation of RV function by echocardiography, there may be inherent issues with its intra- and inter-observer variability compared with RVEF by MRI [23]. However, cardiac serial MRIs could not be justified for clinical and financial reasons based upon current heart failure management strategies, especially when echocardiography could adequately and readily evaluate temporal changes in RV function. The patient cohort were overweight with a mean BMI of 29 kg/m^2. Left ventricular myocardial fibrosis is known to be increased within obese individuals, meaning that this could be a confounding factor within our NICM population, however the impact of obesity and metabolic derangement on the RV myocardium remains unknown [24]. Individual patients likely had adjustments and alterations in their medications during the follow-up phase of the study. Unfortunately, the nature and timing of changes in medications relative to the follow-up echocardiograms cannot be accurately determined retrospectively.

Conclusion

Quantitative assessment of right ventricular structure and function can be technically challenging and is therefore often suboptimal. Cardiac MRI provides a complimentary modality to echocardiography for further right ventricular stratification. This technique is practically feasible, despite the thin right ventricular free wall. CMR functional parameters of RVEF and multi-planar strain imaging provide incremental information regarding global RV dysfunction. This has been previously limited with echocardiography, which is predominantly restricted to assessment of RV 2D longitudinal function and cannot provide accurate assessment of RVEF. The results of this study demonstrate for the first time a proportional relationship between RV function and post-contrast T_1 values, whereby those with worse RVEF had consistently lower post-contrast T_1 values in both the LV and RV. The same relationship did not hold for RVSP as a measure of pulmonary pressures, although associations between both strain and RVSP along with strain and post-contrast T_1 values were demonstrated. These associations between RV function and post-contrast T_1 values support that myocardial fibrosis is a causative factor of RV dysfunction in NICM, irrespective of RV afterload. This same structural milieu also appears integral to the propensity for both positive and negative RV remodeling long-term, suggestive that this is also determined by the degree of underlying RV fibrosis. Additional studies are required to determine if these observations are replicated within other manifestations of RV dysfunction.

References

1. Hinojar R, Varma N, Child N, Goodman B, Jabbour A, Yu CY, Gebker R, Doltra A, Kelle S, Khan S, Rogers T, Arroyo Ucar E, Cummins C, Carr-White G, Nagel E, Puntmann VO (2015) T1 mapping in discrimination of hypertrophic phenotypes: hypertensive heart disease and hypertrophic cardiomyopathy: findings from the international t1 multicenter cardiovascular magnetic resonance study. Circ Cardiovasc Imaging 8(12)
2. Puntmann VO, Voigt T, Chen Z, Mayr M, Karim R, Rhode K, Pastor A, Carr-White G, Razavi R, Schaeffter T, Nagel E (2013) Native t1 mapping in differentiation of normal myocardium from diffuse disease in hypertrophic and dilated cardiomyopathy. JACC Cardiovasc Imaging 6:475–484
3. Jellis C, Wright J, Kennedy D, Sacre J, Jenkins C, Haluska B, Martin J, Fenwick J, Marwick TH (2011) Association of imaging markers of myocardial fibrosis with metabolic and functional disturbances in early diabetic cardiomyopathy. Circ Cardiovasc Imaging 4:693–702
4. Iles L, Pfluger H, Phrommintikul A, Cherayath J, Aksit P, Gupta SN, Kaye DM, Taylor AJ (2008) Evaluation of diffuse myocardial fibrosis in heart failure with cardiac magnetic resonance contrast-enhanced t1 mapping. J Am Coll Cardiol 52:1574–1580
5. Hong YJ, Park CH, Kim YJ, Hur J, Lee HJ, Hong SR, Suh YJ, Greiser A, Paek MY, Choi BW, Kim TH (2015) Extracellular volume fraction in dilated cardiomyopathy patients without obvious late gadolinium enhancement: comparison with healthy control subjects. Int J Cardiovasc Imaging 31(Suppl 1):115–122
6. Burke AP, Farb A, Tashko G, Virmani R (1998) Arrhythmogenic right ventricular cardiomyopathy and fatty replacement of the right ventricular myocardium: are they different diseases? Circulation 97:1571–1580
7. van de Veerdonk MC, Bogaard HJ, Voelkel NF (2016) The right ventricle and pulmonary hypertension. Heart Fail Rev 21(3):259–271
8. La Gerche A, Roberts T, Claessen G (2014) The response of the pulmonary circulation and right ventricle to exercise: exercise-induced right ventricular dysfunction and structural remodeling in endurance athletes (2013 grover conference series). Pulm Circ 4:407–416
9. Puchalski MD, Williams RV, Askovich B, Minich LL, Mart C, Tani LY (2007) Assessment of right ventricular size and function: echo versus magnetic resonance imaging. Congenit Heart Dis 2:27–31
10. Kawel-Boehm N, Dellas Buser T, Greiser A, Bieri O, Bremerich J, Santini F (2014) In-vivo assessment of normal t1 values of the right-ventricular myocardium by cardiac mri. Int J Cardiovasc Imaging 30:323–328
11. Platts D, Brown M, Javorsky G, West C, Kelly N, Burstow D (2010) Comparison of fluoroscopic versus real-time three-dimensional transthoracic echocardiographic guidance of endomyocardial biopsies. Eur J Echocardiogr 11:637–643
12. Aquaro GD, Camastra G, Monti L, Lombardi M, Pepe A, Castelletti S, Maestrini V, Todiere G, Masci P, di Giovine G, Barison A, Dellegrottaglie S, Perazzolo Marra M, Pontone G, Di Bella G (2016) Reference values of cardiac volumes, dimensions, and new functional parameters by MR: a multicenter, multivendor study. J Magn Reson Imaging 45(4):1055–1067
13. Foppa M, Arora G, Gona P, Ashrafi A, Salton CJ, Yeon SB, Blease SJ, Levy D, O'Donnell CJ, Manning WJ, Chuang ML (2016) Right ventricular volumes and systolic function by cardiac magnetic resonance and the impact of sex, age, and obesity in a longitudinally followed cohort free of pulmonary and cardiovascular disease: the framingham heart study. Circ Cardiovasc Imaging 9:e003810
14. Gai N, Turkbey EB, Nazarian S, van der Geest RJ, Liu CY, Lima JA, Bluemke DA (2011) T1 mapping of the gadolinium-enhanced myocardium: adjustment for factors affecting interpatient comparison. Magn Reson Med 65:1407–1415
15. Puntmann VO, Carr-White G, Jabbour A, Yu CY, Gebker R, Kelle S, Hinojar R, Doltra A, Varma N, Child N, Rogers T, Suna G, Arroyo Ucar E, Goodman B, Khan S, Dabir D, Herrmann E, Zeiher AM, Nagel E (2016) T1-mapping and outcome in nonischemic cardiomyopathy: all-cause mortality and heart failure. JACC Cardiovasc Imaging 9:40–50
16. Rudski LG, Lai WW, Afilalo J, Hua L, Handschumacher MD, Chandrasekaran K, Solomon SD, Louie EK, Schiller NB (2010) Guidelines for the echocardiographic assessment of the right heart in adults: a report from the american society of echocardiography endorsed by the european association of echocardiography, a registered branch of the european society of cardiology, and the canadian society of echocardiography. J Am Soc Echocardiogr 23:685–713
17. Dabir D, Child N, Kalra A, Rogers T, Gebker R, Jabbour A, Plein S, Yu CY, Otton J, Kidambi A, McDiarmid A, Broadbent D, Higgins DM, Schnackenburg B, Foote L, Cummins C, Nagel E, Puntmann VO (2014) Reference values for healthy human myocardium using a t1 mapping methodology: results from the international t1 multicenter cardiovascular magnetic resonance study. J Cardiovasc Magn Reson 16:69
18. Freed BHSE, Benefield BC, Spottiswoode B, Brady C, Allen B, Shah SJ, Carr JC, Markl M, Collins JD (2016) Right ventricular t1 mapping: a feasibility study. J Heart Lung Transplant 35:S275–S276
19. Garcia-Lunar IPP, Pozo E, Calcagno C, Ramachandran S, Adapoe CM, Nair A, Jacobi A, Fuster V, Sanz J (2013) Myocardial fibrosis with t1 mapping and right ventricular performance in pulmonary hypertension. J Cardiovasc Magn Reson 15(Suppl 1):E102
20. Gardner BI, Bingham SE, Allen MR, Blatter DD, Anderson JL (2009) Cardiac magnetic resonance versus transthoracic echocardiography for the assessment of cardiac volumes and regional function after myocardial infarction: an intrasubject comparison using simultaneous intrasubject recordings. Cardiovasc Ultrasound 7:38
21. Farsalinos KE, Daraban AM, Unlu S, Thomas JD, Badano LP, Voigt JU (2015) Head-to-head comparison of global longitudinal strain measurements among nine different vendors: the EACVI/ASE inter-vendor comparison study. J Am Soc Echocardiogr 28:1171–1181, e1172
22. Yingchoncharoen T, Jellis C, Popovic ZB, Wang L, Gai N, Levy WC, Tang WH, Flamm S, Kwon DH (2016) Focal fibrosis and diffuse fibrosis are predictors of reversed left ventricular remodeling in patients with non-ischemic cardiomyopathy. Int J Cardiol 221:498–504
23. Lemarie J, Huttin O, Girerd N, Mandry D, Juilliere Y, Moulin F, Lemoine S, Beaumont M, Marie PY, Selton-Suty C (2015) Usefulness of speckle-tracking imaging for right ventricular assessment after acute myocardial infarction: a magnetic resonance imaging/echocardiographic comparison within the relation between aldosterone and cardiac remodeling after myocardial infarction study. J Am Soc Echocardiogr 28:818–827 e814
24. Wong C, Marwick TH (2007) Obesity cardiomyopathy: pathogenesis and pathophysiology. Nat Clin Pract Cardiovasc Med 4:436–443